New Journal of Physics
The open access journal at the forefront of physics

Deutsche Physikalische Gesellschaft DPG IOP Institute of Physics International Year of Quantum Science and Technology

OPEN ACCESS

Simultaneous cooling and entanglement of mechanical modes of a micromirror in an optical cavity

To cite this article: Claudiu Genes *et al* 2008 *New J. Phys.* **10** 095009

View the article online for updates and enhancements.

You may also like

- Thermal-noise-resistant entanglement and steering via dark-mode engineering in multimode optomechanical system
Ping-Chi Ge, Yikyung Yu, Hao-Tian Wu et al.
- Anti-correlated phonons with two-mode Gaussian squeezed state
X Y Zhang, Y H Zhou, Y Q Guo et al.
- Dynamics of Rényi-2 correlations in optomechanics
Abderrahim Lakhfif, Abdelkader Hidki, Jamal El Qars et al.

This content was downloaded from IP address 130.186.31.178 on 24/07/2025 at 09:18

New Journal of Physics
The open-access journal for physics

Simultaneous cooling and entanglement of mechanical modes of a micromirror in an optical cavity

Claudiu Genes, David Vitali[1] and Paolo Tombesi
Dipartimento di Fisica, Università di Camerino, I-62032 Camerino, Italy
E-mail: david.vitali@unicam.it

New Journal of Physics **10** (2008) 095009 (18pp)
Received 15 March 2008
Published 30 September 2008
Online at http://www.njp.org/
doi:10.1088/1367-2630/10/9/095009

Abstract. Laser cooling of a mechanical mode of a resonator by the radiation pressure of a detuned optical cavity mode has been recently demonstrated by various groups in different experimental configurations. Here, we consider the effect of a second mechanical mode with a close but different resonance frequency. We show that the nearby mechanical resonance is simultaneously cooled by the cavity field, provided that the difference between the two mechanical frequencies is not too small. When this frequency difference becomes smaller than the effective mechanical damping of the secondary mode, the two cooling processes interfere destructively similarly to what happens in electromagnetically induced transparency, and cavity cooling is suppressed in the limit of identical mechanical frequencies. We show that also the entanglement properties of the steady state of the tripartite system crucially depend upon the difference between the two mechanical frequencies. If the latter is larger than the effective damping of the second mechanical mode, the state shows fully tripartite entanglement and each mechanical mode is entangled with the cavity mode. If instead, the frequency difference is smaller, the steady state is a two-mode biseparable state, inseparable only when one splits the cavity mode from the two mechanical modes. In this latter case, the entanglement of each mechanical mode with the cavity mode is extremely fragile with respect to temperature.

[1] Author to whom any correspondence should be addressed.

© IOP Publishing Ltd and Deutsche Physikalische Gesellschaft

Contents

1. Introduction 2
2. System dynamics 3
3. Simultaneous cooling 6
4. Entanglement properties of the steady state of the system 12
5. Classification of tripartite entanglement 15
6. Conclusions 16
Acknowledgment 16
References 17

1. Introduction

Mechanical resonators at the micro- and nanometer scales are now widely employed in the highly sensitive detection of mass and forces [1]. Among the applications that have become possible are measurements of forces between individual biomolecules [2], forces arising from magnetic resonance of single spins [3], and perturbations that arise from mass fluctuations involving single atoms and molecules [4]. The recent improvements in nanofabrication techniques suggest that in the near future these devices will reach the regime in which their sensitivity will be limited by the ultimate quantum limits set by the Heisenberg principle, as suggested earlier in the context of the detection of gravitational waves by the pioneering work of Braginsky and coworkers [5]. An important step in this direction would be to show cooling of such microresonators to their quantum ground state. It would represent a remarkable signature of the quantum behavior of a macroscopic object, allowing further shedding of light on the quantum–classical boundary [6]. Recent experiments achieved promising results via cryogenic cooling [7], via back-action cooling, in which the off-resonant operation of the cavity results in a retarded back action on the mechanical system [8]–[13], or by cold-damping quantum feedback where the oscillator position is measured through a phase-sensitive detection of the cavity output and the resulting photocurrent is used for a real-time correction of the dynamics [14]–[18]. As shown by recent theoretical results [19]–[26], these cooling schemes are in principle capable of bringing the microresonator down to its ground state. Both mechanisms achieve cooling by increasing the damping of the mechanical resonator, so that it becomes insensitive to thermal noise. It is important to analyze all the possible limitations of ground state cooling, also because this would open up the experimental realization to a number of genuine quantum phenomena, such as the possibility of entangling an acoustic mode with a cavity quantum field [27], or with another mechanical oscillator [28]–[31], and even continuous variable quantum information protocols such as quantum teleportation [32], and entanglement swapping [33].

Here, we shall consider only back-action cooling and the prototypical situation of an optical Fabry–Perot cavity with a rigid massive mirror at one end and a lighter, vibrating mirror at the opposite end. An intense laser beam drives a single, well-separated, cavity mode which excites many internal vibrational modes of the oscillating mirror, via the radiation pressure. Apart from recent particular examples [31, 34], theoretical treatments of back-action cooling have to date focused on a single cavity mode–*single mechanical mode* interaction, which is

justified when a bandpass filter in the detection scheme is used, because coupling between the different vibrational modes is typically negligible.

In this paper, we extend the treatment of cooling by including the effect of secondary acoustic modes whose resonance frequency is not far from that of the mechanical mode of interest, so that they cannot be neglected and filtered out by the detection process. We specialize to the case of a single additional mode and study its effect on cooling and on entanglement properties of the steady state of the system. We find that cooling of the main mode crucially depends upon the difference between the two mechanical resonance frequencies. If this difference is larger than the effective damping of the secondary mode, cooling is not crucially affected by the presence of the adjacent mode, and the cavity mode is capable of *simultaneously cooling* the nearby mechanical mode close to its ground state. In this regime, the cavity mode is entangled with each mechanical mode and the stationary state shows fully tripartite entanglement. If instead, the two mechanical frequencies are closer than the effective mechanical damping, then the two cooling processes interfere destructively and neither mechanical mode is cooled. This destructive interference also affects the stationary entanglement, which becomes extremely fragile with respect to temperature. The steady state of the system becomes a two-mode biseparable state, (i.e. of 'class 3' [35]), which means inseparable only when one splits the cavity mode from the two mechanical modes.

This paper is structured as follows. Section 2 introduces the physics of the optomechanical interaction inside an optical cavity and the linearized Langevin equations formalism. In section 3, we solve the dynamics of two mechanical modes coupled to the cavity field and compare it to the case of a single mechanical mode. In sections 4 and 5, we characterize the simultaneous entanglement of the two acoustic modes with the cavity field and study the tripartite entanglement of the steady states, respectively. Section 6 concludes the paper.

2. System dynamics

We consider an optical Fabry–Perot cavity of length L formed by a rigid massive mirror at one end and a vibrating micromechanical mirror at the opposite end, driven by a laser with frequency ω_0. We shall refer from now on to this prototypal situation, even though the analysis could be easily adapted to other cavity geometries, such as the toroidal silica microcavities described in [10, 13]. The laser significantly drives only a single cavity mode with frequency ω_c, from which it is detuned by $\Delta_0 = \omega_c - \omega_0$. The motion of the micro-mirror can be described by the set of its vibrational normal modes, each with its own resonance frequency ω_j and damping rate γ_j. The Hamiltonian of the system is

$$H = \hbar\omega_c a^\dagger a + \sum_j \frac{\hbar\omega_j}{2}(p_j^2 + q_j^2) + H_{\rm int} + i\hbar E(a^\dagger e^{-i\omega_0 t} - a e^{i\omega_0 t}), \tag{1}$$

where the cavity field annihilation operator a satisfies the commutation relation $[a, a^\dagger] = 1$, and the mechanical modes are described by dimensionless position and momentum operators satisfying $[q_k, p_j] = i\delta_{kj}$. Denoting the cavity decay rate by κ, the parameter E is related to the input power $\mathcal{P}_{\rm in}$ by $|E| = \sqrt{2\mathcal{P}_{\rm in}\kappa/\hbar\omega_0}$. The single cavity mode description is valid in the adiabatic limit when all the relevant mechanical frequencies ω_j are much smaller than the cavity free spectral range $c/2L$, which is typically satisfied for small cavities. In this limit, the scattering of photons by the mirror motion from the driven mode into other cavity modes is negligible [36]. The interaction between the cavity mode and the vibrational modes is described

by $H_{\rm int}$, and it is due to the radiation pressure acting on the surface S of the vibrating mirror. One has [37]

$$H_{\rm int} = -\int_S \mathrm{d}^2 r\, \vec{P}(\vec{r}) \cdot \vec{u}(\vec{r}), \tag{2}$$

where $\vec{P}(\vec{r})$ is the radiation pressure field and

$$\vec{u}(\vec{r}) = \sum_j \sqrt{\frac{\hbar}{m_j \omega_j}} q_j \vec{u}_j(\vec{r}) \tag{3}$$

is the displacement field of the mirror surface at point $\vec{r}$. This field can be written as a sum over the corresponding (dimensionless) displacement field of each normal mode, $\vec{u}_j(\vec{r})$, which is characterized by an effective mass $m_j = \rho \int \mathrm{d}^3 r |\vec{u}_j(\vec{r})|^2$ (ρ the mirror mass density). We consider a one-dimensional situation, i.e. we assume that the driving laser and the cavity are perfectly aligned. In this case, light is sensitive only to mirror surface deformations along the cavity axis, $u_x(\vec{r})$, so that equation (2) becomes

$$H_{\rm int} = -\int_S \mathrm{d}^2 r\, P_x(\vec{r}) u_x(\vec{r}). \tag{4}$$

In general, the radiation pressure due to an optical power $\mathcal{P}$ impinging on a mirror with reflection coefficient $\mathcal{R}$ can be written as

$$P_x(\vec{r}) = \frac{2\mathcal{P}}{c} \mathcal{R} v_{\rm opt}^2(\vec{r}), \tag{5}$$

with $v_{\rm opt}(\vec{r})$ denoting the spatial structure of the incident optical field on the mirror surface. Within the cavity, one can rewrite $2\mathcal{P}/c = \hbar(\omega_{\rm c}/L) a^\dagger a$ and also assume $\mathcal{R} \simeq 1$. One ends up with

$$H_{\rm int} = -\hbar \sum_j G_0^j a^\dagger a q_j, \tag{6}$$

where the optomechanical couplings are given by

$$G_0^j = \frac{\omega_{\rm c} c_j}{L} \sqrt{\frac{\hbar}{m_j \omega_j}}, \tag{7}$$

and

$$c_j = \int_S \mathrm{d}^2 r\, v_{\rm opt}^2(\vec{r}) (u_j)_x(\vec{r}) \tag{8}$$

is the overlap at the mirror surface between the cavity mode and the jth mechanical mode. Due to the chosen normalization of $v_{\rm opt}^2(\vec{r})$ and $\vec{u}_j(\vec{r})$, the overlaps satisfy the condition $0 \leqslant c_j \leqslant 1$. Equations (6) and (7) show that the radiation pressure directly couples the cavity mode only with the mirror collective displacement operator $q_{\rm eff} = \sum_j G_0^j q_j$. When the detection bandwidth involves only a single, isolated, vibrational normal mode of the microresonator, the collective coordinate $q_{\rm eff}$ is well approximated by the selected normal mode, and the single harmonic oscillator description usually adopted is justified. In the more general case, one has to include in the dynamical description of the system all the vibrational normal modes which contribute to the detected signal.

The unavoidable action of damping and noise on the dynamics associated with the Hamiltonian of equation (1) is described by adopting the formalism of quantum Langevin equations [38, 39] which, in the frame rotating at the laser frequency ω_0, are given by

$$\dot{q}_j = \omega_j p_j, \tag{9}$$

$$\dot{p}_j = -\omega_j q_j - \gamma_j p_j + G_0^j a^\dagger a + \xi_j, \tag{10}$$

$$\dot{a} = -(\kappa + \mathrm{i}\Delta_0)a + \mathrm{i}\sum_j G_0^j a q_j + E + \sqrt{2\kappa}a^{\mathrm{in}}. \tag{11}$$

The cavity input noise is delta correlated in the time domain $\langle a^{\mathrm{in}}(t)a^{\mathrm{in},\dagger}(t')\rangle = \delta(t-t')$, while the mechanical Brownian stochastic forces with zero mean value $\xi_j(t)$ are uncorrelated with each other and have the following, generally non-Markovian, correlation functions

$$\langle \xi_k(t)\xi_j(t')\rangle = \delta_{kj}\frac{\gamma_j}{2\pi\omega_j}\int \mathrm{d}\omega\, \mathrm{e}^{-\mathrm{i}\omega(t-t')}\omega\left[\coth\left(\frac{\hbar\omega}{2k_{\mathrm{B}}T}\right)+1\right] \tag{12}$$

with k_{B} the Boltzmann constant and T the temperature of the reservoir of the micromechanical mirror. However, the involved mechanical frequencies are never larger than hundreds of MHz and therefore, as discussed in [25] (see also [40]), even for cryogenic temperatures one can make the approximation

$$\frac{\gamma_j\omega}{\omega_j}\coth\left(\frac{\hbar\omega}{2k_{\mathrm{B}}T}\right) \simeq \gamma_j\frac{2k_{\mathrm{B}}T}{\hbar\omega_j} \simeq \gamma_j\left(2n_j+1\right), \tag{13}$$

where $n_j = [\exp\{\hbar\omega_j/k_{\mathrm{B}}T\}-1]^{-1}$ is the mean thermal phonon number of mode j. As a consequence, the Brownian noise can be safely considered Markovian, that is,

$$\left\langle \xi_k(t)\xi_j(t')\right\rangle \simeq \delta_{kj}\gamma_j\left[(2n_j+1)\delta(t-t')+\mathrm{i}\frac{\delta'(t-t')}{\omega_j}\right], \tag{14}$$

where $\delta'(t-t')$ denotes the derivative of the Dirac delta.

Ground-state cooling is typically achieved when the radiation pressure coupling is strong. This can be obtained when the intracavity field is very intense, i.e. for high-finesse cavities and enough driving power. In this limit (and if the system is stable), the system is characterized by a semiclassical steady state with the cavity mode in a coherent state with amplitude α_{s} ($|\alpha_{\mathrm{s}}| \gg 1$), and a new equilibrium position for the vibrational modes, displaced by q_{s}^j. The parameters α_{s} and q_{s}^j are the solutions of the nonlinear algebraic equations obtained by factorizing equations (9)–(11) and setting the time derivatives to zero. They are given by

$$q_{\mathrm{s}}^j = \frac{G_0^j|\alpha_{\mathrm{s}}|^2}{\omega_j}, \tag{15}$$

$$p_{\mathrm{s}}^j = 0, \tag{16}$$

$$\alpha_{\mathrm{s}} = \frac{E}{\kappa + \mathrm{i}\Delta_{(N)}}, \tag{17}$$

where the effective detuning $\Delta_{(N)}$ is obtained from Δ_0 by subtracting the frequency shift caused by the steady-state radiation pressure

$$\Delta_{(N)} = \Delta_0 - |\alpha_{\mathrm{s}}|^2\sum_j\frac{[G_0^j]^2}{\omega_j}. \tag{18}$$

Then, we linearize equations (9)–(11) around the steady-state values by writing operators as sums of averages plus fluctuations: $a = \alpha_s + \delta a$, $q_j = q_s^j + \delta q_j$ and $p_j = p_s^j + \delta p_j$. The nonlinear terms $\delta a^\dagger \delta a$ and $\delta a \delta q_j$ can be ignored when the fluctuations are much smaller than the mean value, and this is certainly satisfied when $|\alpha_s| \gg 1$. One therefore arrives at a system of linearized quantum Langevin equations

$$\delta \dot{q}_j = \omega_j \delta p_j, \tag{19}$$

$$\delta \dot{p}_j = -\omega_j \delta q_j - \gamma_j \delta p_j + G_j \delta X + \xi_j, \tag{20}$$

$$\delta \dot{X} = -\kappa \delta X + \Delta_{(N)} \delta Y + \sqrt{2\kappa} X^{\text{in}}, \tag{21}$$

$$\delta \dot{Y} = -\kappa \delta Y - \Delta_{(N)} \delta X + \sum_j G_j \delta q_j + \sqrt{2\kappa} Y^{\text{in}}. \tag{22}$$

We have chosen the phase reference of the cavity field so that α_s is real and positive, we have defined the field quadratures $\delta X \equiv (\delta a + \delta a^\dagger)/\sqrt{2}$ and $\delta Y \equiv (\delta a - \delta a^\dagger)/\mathrm{i}\sqrt{2}$ and the corresponding Hermitian input noise quadratures $X^{\text{in}} \equiv (a^{\text{in}} + a^{\text{in},\dagger})/\sqrt{2}$ and $Y^{\text{in}} \equiv (a^{\text{in}} - a^{\text{in},\dagger})/\mathrm{i}\sqrt{2}$. We have also defined the effective optomechanical couplings

$$G_j = G_0^j \alpha_s \sqrt{2} = \frac{2\omega_c c_j}{L} \sqrt{\frac{\mathcal{P}_{\text{in}} \kappa}{m_j \omega_j \omega_0 \left(\kappa^2 + \Delta_{(N)}^2\right)}}. \tag{23}$$

3. Simultaneous cooling

At the steady state, the energy of each mechanical mode can be written in terms of the variances of the corresponding position and momentum operators,

$$U_j = \frac{\hbar \omega_j}{2} \left[\left\langle \delta q_j^2 \right\rangle + \left\langle \delta p_j^2 \right\rangle\right]. \tag{24}$$

In the absence of any cooling mechanism, one has $U_j = \hbar \omega_j (n_j + 1/2)$ and therefore when cooling occurs we can write $U_j = \hbar \omega_j (n_j^{\text{eff}} + 1/2)$, where n_j^{eff} is the mean effective excitation number of the j mode, corresponding to an effective mode temperature $T_j^{\text{eff}} = \hbar \omega_j / [k_B \ln(1 + 1/n_j^{\text{eff}})]$. If one defines the vector of fluctuations

$$u(t) = \left(\delta q_1(t), \delta p_1(t), \ldots \delta q_j(t), \delta p_j(t) \ldots, \delta X(t), \delta Y(t)\right)^\intercal, \tag{25}$$

and the vector of noises

$$v(t) = \left(0, \xi_1(t), \ldots 0, \xi_j(t) \ldots, \sqrt{2\kappa} X^{\text{in}}(t), \sqrt{2\kappa} Y^{\text{in}}(t)\right)^\intercal, \tag{26}$$

then equations (19)–(22) can be written in a compact form as

$$\frac{\mathrm{d}}{\mathrm{d}t} u(t) = A_{(N)} u(t) + v(t), \tag{27}$$

where $A_{(N)}$ is the drift matrix that governs the dynamics of the expectation values. Since the evolution is linear and the noise terms in equations (19)–(22) are zero-mean quantum Gaussian noises, the steady state of the fluctuations is a zero-mean multipartite Gaussian state fully characterized by its correlation matrix $\mathcal{V}$, whose elements are defined as

$$\mathcal{V}_{lm} = \frac{\langle u_l(\infty) u_m(\infty) + u_m(\infty) u_l(\infty) \rangle}{2}. \tag{28}$$

Using standard techniques [41], one can determine the steady-state correlation matrix $\mathcal{V}$ by solving the Lyapunov equation

$$A_{(N)}\mathcal{V}+\mathcal{V}A_{(N)}^{\mathsf{T}}=-D, \tag{29}$$

where

$$D=\mathrm{diag}\left[0,\gamma_1(2\bar{n}_1+1),\ldots 0,\gamma_j(2\bar{n}_j+1),\ldots\kappa,\kappa\right], \tag{30}$$

is the diagonal $(2N+2)\times(2N+2)$ diffusion matrix determined by the noise correlation functions. The stationary variances of the mechanical modes are given by the corresponding diagonal matrix elements of $\mathcal{V}$.

If only one mechanical mode is considered, the drift matrix assumes the following form

$$A_{(1)}=\begin{pmatrix}0 & \omega_1 & 0 & 0\\ -\omega_1 & -\gamma_1 & G_1 & 0\\ 0 & 0 & -\kappa & \Delta_{(1)}\\ G_1 & 0 & \Delta_{(1)} & -\kappa\end{pmatrix}, \tag{31}$$

where $\Delta_{(1)}=\Delta_0-G_1^2/2\omega_1$ is the effective single-mode detuning. The stationary variances are given by $\langle\delta q_1^2\rangle=\mathcal{V}_{11}$ and $\langle\delta p_1^2\rangle=\mathcal{V}_{22}$ and their exact expression is given in [25], wherein they have been obtained by integrating the spectra obtained from the Fourier transformation of the quantum Langevin equations. The two calculations coincide whenever a Markovian treatment of the quantum Brownian noise acting on the mechanical modes is made, i.e. when the approximation of equation (13) is considered.

As shown in [23]–[26], cooling occurs when $\Delta_{(1)}\simeq\omega_1$, i.e. when the laser is red-detuned with respect to the cavity mode, and the latter is resonant with the anti-Stokes sideband of the laser. In fact, the laser light is scattered by the oscillating mirror into the Stokes and anti-Stokes sidebands with frequencies $\omega_0\pm\omega_1$. The generation of an anti-Stokes photon takes away a vibrational phonon and is responsible for cooling, while the generation of a Stokes photon heats the mirror by producing an extra phonon. If the cavity is resonant with the anti-Stokes sideband, cooling prevails and one has a positive net laser cooling rate Γ given by the difference of the scattering rates, $\Gamma=A_--A_+$. It is also shown in [23]–[26] that laser cooling is optimized and can approach ground-state cooling in the resolved band limit, when $\kappa<\omega_1$ (actually when $\kappa\simeq 0.2\omega_1$ [23, 25]). Another important condition for ground-state cooling is to have large optomechanical coupling G_1, which is obtained for large intracavity power. However, G_1 has an upper bound imposed by the stability conditions [42], which in the case of a single mechanical mode and restricted to positive $\Delta_{(1)}$, reduces to the single inequality [25, 27],

$$\eta^{(1)}=1-\frac{G_1^2\Delta_{(1)}}{\omega_1(\kappa^2+\Delta_{(1)}^2)}>0. \tag{32}$$

However, as we have seen in section 2, the optical mode is always coupled to *all* the mechanical modes with a nonzero overlap c_j with the cavity mode at the mirror surface. Therefore, the actual stability conditions of the system are determined by the coupling with *all* the N excited mechanical modes, even the unobserved ones. By applying the Routh–Hurwitz criterion [42], it is possible to see that, if we restrict to the cooling regime of positive detunings $\Delta_{(N)}$, there is always one nontrivial stability condition only, which is the direct N-mode generalization of equation (32),

$$\eta^{(N)}=1-\frac{\Delta_{(N)}}{\kappa^2+\Delta_{(N)}^2}\sum_j\frac{G_j^2}{\omega_j}>0. \tag{33}$$

The violation of this condition leads to bistable behavior, which has been experimentally verified in [43]. We shall assume that this stability condition is always satisfied from now on.

In the case of two mechanical modes, the drift matrix is

$$A_{(2)} = \begin{pmatrix} 0 & \omega_1 & 0 & 0 & 0 & 0 \\ -\omega_1 & -\gamma_1 & 0 & 0 & G_1 & 0 \\ 0 & 0 & 0 & \omega_2 & 0 & 0 \\ 0 & 0 & -\omega_2 & -\gamma_2 & G_2 & 0 \\ 0 & 0 & 0 & 0 & -\kappa & \Delta_{(2)} \\ G_1 & 0 & G_2 & 0 & \Delta_{(2)} & -\kappa \end{pmatrix} \tag{34}$$

We have exactly solved the Lyapunov equation (29) and analyzed the stationary position and momentum variances of the two mechanical modes in a parameter regime close to that of optimal cooling for a single mode, in order to see if and how the secondary mechanical mode affects ground-state cooling. The results are shown in figure 1, where the effective phonon number $n_{\rm eff}$ of the main mode (blue line) and of the secondary mode (green line) are plotted and compared to the single-mode cooling case (red line). We have considered experimentally feasible parameters (see caption), i.e. mechanical quality factors of the order of 10^5 and resonance frequency of the main mode $\omega_1/2\pi = 10\,\mathrm{MHz}$.

We find two different situations, depending upon the value of the difference between the two mechanical frequencies, $\delta\omega_{21} = \omega_2 - \omega_1$. Figures 1(a) and (b) refer to the case when the two frequencies are quite distinct, $\omega_2 = 1.7\omega_1$ in (a) and $\omega_2 = 2\omega_1$ in (b), and they plot $n_{\rm eff}$ versus the effective cavity detuning $\Delta_{(2)} = \Delta_0 - G_1^2/2\omega_1 - G_2^2/2\omega_2 = \Delta_{(1)} - G_2^2/2\omega_2$. Figure 1(a) refers to the good cavity limit, $\kappa \simeq 0.2\omega_1$, corresponding to a cavity finesse $\mathcal{F} = 1.5 \times 10^5$, while figure 1(b) refers to a larger cavity bandwidth, $\kappa \simeq \omega_1$, corresponding to a finesse $\mathcal{F} = 3 \times 10^4$. We consider a reservoir temperature $T = 0.6\,\mathrm{K}$, oscillators with mass $m = 250\,\mathrm{ng}$ and a cavity length $L = 1\,\mathrm{mm}$. The results show that, when the two mechanical modes are well separated ($\delta\omega_{21} \simeq \omega_1$), the nearby mode does not disturb the cooling of the mechanical mode of interest, as witnessed by the perfect overlap of the blue and red curves, both in (a) and in (b). Even better, the secondary mode is *simultaneously* cooled close to its ground state (green curve). The comparison between figures 1(a) and (b) show that simultaneous cooling is influenced by the value of the cavity bandwidth κ. In fact, the interval for the detuning $\Delta_{(2)}$ within which one has a significantly low value of $n_{\rm eff}$ is given by $\omega_j - \kappa \lesssim \Delta_{(2)} \lesssim \omega_j + \kappa$, as can be seen from the width of the peak of the net laser cooling rate for mode j [23]–[26],

$$\Gamma_j = \frac{2G_j^2\Delta_{(2)}\omega_j\kappa}{\left[\kappa^2 + (\omega_j - \Delta_{(2)})^2\right]\left[\kappa^2 + (\omega_j + \Delta_{(2)})^2\right]} \tag{35}$$

as a function of $\Delta_{(2)}$. Therefore, if the difference between the two mechanical frequencies is larger than κ, the two modes are optimally cooled at two well-distinct values of $\Delta_{(2)}$ and one can efficiently cool both modes only by fixing the detuning within a very narrow interval halfway between the two mechanical resonances, $\Delta_{(2)} \simeq (\omega_1 + \omega_2)/2$ (see figure 1(a)). However, due to the small value of κ, the achievable value of $n_{\rm eff}$ at this intermediate detuning is appreciably larger ($n_{\rm eff} \simeq 0.5$) than the optimal one achievable, if one wanted to cool only one mode ($n_{\rm eff} \simeq 0.15$). Instead, for a larger cavity bandwidth, $\kappa \simeq \delta\omega_{21}$, good simultaneous cooling of both modes is achievable in a significantly wider interval of detunings $\Delta_{(2)}$ (see figure 1(b)).

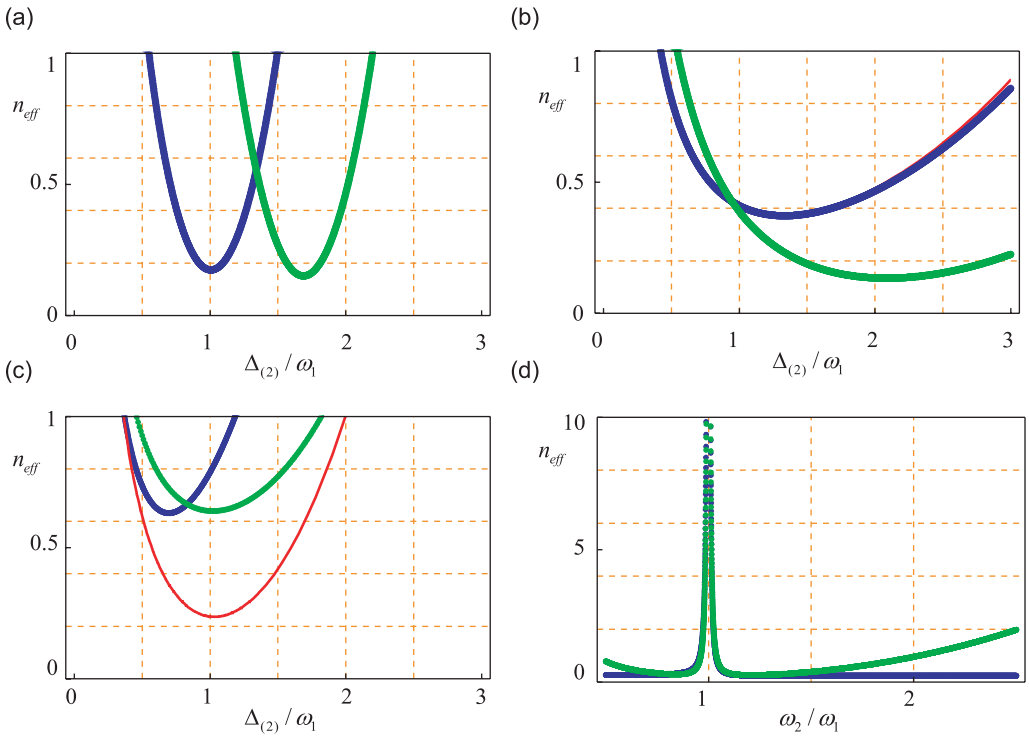

Figure 1. (a) Simultaneous cooling of two acoustic modes (blue line: main mode, green line: secondary mode) of a single mirror versus normalized detuning $\Delta_{(2)}/\omega_1$. The mechanical parameters are: $\gamma_1/2\pi = \gamma_2/2\pi = 100\,\text{Hz}$, $\omega_1/2\pi = 10\,\text{MHz}$, $\omega_2 = 1.7 \times \omega_1$, $m_1 = m_2 = 250\,\text{ng}$ and $T = 0.6\,\text{K}$, that corresponds to initial occupancies $n_1 = 1250$ and $n_2 = 735$. The cavity of length $L = 1\,\text{mm}$ and finesse $\mathcal{F} = 1.5 \times 10^5$ is driven by a laser of wavelength $\lambda_0 = 1064\,\text{nm}$ and power $P_0 = 30\,\text{mW}$ (at $\Delta_{(2)} = \omega_1$), which gives $\kappa \simeq G_1 \simeq \omega_1/5$. A red line is plotted but not visible owing to its almost complete overlap with the blue line, that portrays the behavior of the main mode cooling in the absence of the secondary mode. The final effective temperatures achieved are $T_1^{\text{eff}} \simeq 0.24\,\text{mK}$ and $T_2^{\text{eff}} \simeq 0.42\,\text{mK}$. At the intersection of the cooling curves, the effective temperatures are $T_1^{\text{eff}} \simeq 0.46\,\text{mK}$ and $T_2^{\text{eff}} \simeq 0.79\,\text{mK}$. (b) Simultaneous cooling for a smaller cavity finesse $\mathcal{F} = 3 \times 10^4$ (corresponding to $\kappa \simeq \omega_1$) and $P = 100\,\text{mW}$ (that gives $G_1 = 0.6 \times \omega_1$). The main mode is chosen as before and its independent cooling curve is shown in red (again the two curves for n_{eff} overlap almost everywhere), while the secondary mode is fixed at frequency $\omega_2 = 2\omega_1$. (c) Simultaneous cooling for closely spaced modes $\omega_2 = 0.95 \times \omega_1$ and parameters $\kappa \simeq \omega_1/2$, $G_1 \simeq 0.3 \times \omega_1$. The cooling curve of the main mode (blue line) in the presence of the secondary mode (green line) is quite different from the independent cooling curve (red line). (d) For the same parameters as in (c) the occupancy of both the modes at $\Delta_{(2)} = \omega_1$ is shown versus ω_2/ω_1. An optimal occupancy of 0.22 is reached for well-separated frequencies, but it is strongly disturbed around $\omega_2/\omega_1 \simeq 1$. When the two frequencies are equal, cooling is practically absent.

Figures 1(c) and (d) show that the situation is very different when the two mechanical resonances get very close. Figure 1(c) refers to $\omega_2 = 0.95 \times \omega_1$, and one can see that in this case the occupancies $n_{\rm eff}$ of the two modes are appreciably higher than the one corresponding to a single isolated mode (red line). This means that when $\delta\omega_{21}$ is small enough, the two cooling processes tend to interfere destructively. This is clearly confirmed by figure 1(d), where $n_{\rm eff}$ at the fixed optimal detuning $\Delta_{(2)} = \omega_1$ is plotted versus the ratio ω_2/ω_1; an occupancy of $n_{\rm eff} = 0.22$ is reached for well-separated frequencies, but both modes are practically uncooled in a small interval around $\omega_2/\omega_1 \simeq 1$.

This fact, at first sight unexpected, can be explained in terms of classical destructive interference between two resonant oscillators. A first explanation can be obtained by looking at the mechanical susceptibility of the main oscillator in the presence of the second mode, $\chi_1^{\rm tm}(\omega)$. It can be derived by Fourier transforming the quantum Langevin equations, and is given by

$$\left[\chi_1^{\rm tm}(\omega)\right]^{-1} = \left[\chi_1(\omega)\right]^{-1} - \chi_2(\omega) z^2(\omega) G_1^2 G_2^2, \tag{36}$$

where

$$z(\omega) = \frac{\Delta}{(\kappa - {\rm i}\omega)^2 + \Delta^2}, \tag{37}$$

$$\left[\chi_i(\omega)\right]^{-1} = \left[\chi_0^1(\omega)\right]^{-1} - z(\omega) G_i^2, \qquad i = 1, 2 \tag{38}$$

is the susceptibility of mode i modified by the radiation pressure of the cavity field, in the absence of the other mode, and

$$\left[\chi_0^i(\omega)\right]^{-1} = \frac{1}{\omega_i}\left[(\omega_i^2 - \omega^2) - {\rm i}\omega\gamma_i\right] \tag{39}$$

is the bare susceptibility of the isolated microresonator. One can get an intuitive idea of the response of the mechanical mode of interest by rewriting $\chi_1^{\rm tm}(\omega)$ as the susceptibility of a harmonic oscillator with frequency-dependent resonance frequency $\omega_i^{\rm eff}(\omega)$ and damping $\gamma_i^{\rm eff}(\omega)$,

$$\left[\chi_1^{\rm tm}(\omega)\right]^{-1} = \frac{1}{\omega_i}\left[\left(\omega_i^{\rm eff}(\omega)^2 - \omega^2\right) - {\rm i}\omega\gamma_i^{\rm eff}(\omega)\right]. \tag{40}$$

These two functions in the case of mode 1 are plotted in figure 2 for the case of identical mechanical frequencies, $\omega_1 = \omega_2$. In this case, both the effective damping and the effective frequency are strongly modified by the presence of the second mode (blue curve). The modification of the mechanical frequency due to radiation pressure is the so-called 'optical spring effect', which may lead to significant frequency shifts in the case of low-frequency oscillators [11], but does not have significant effects in the case of higher frequencies, such as those described in [8]–[10], and assumed here (see figure 2(b)). What is relevant is the modification of the effective damping that, in the presence of the second mode, quickly drops to a very small value in a narrow interval around resonance. Since cooling is signaled by an increased mechanical damping, this drop is just a manifestation of the suppression of cooling taking place when the two mechanical modes are resonant (see figure 2(a)). This behavior is well described by the analytic expression of the effective frequency-dependent damping $\gamma_i^{\rm eff}(\omega)$. The latter assumes a simple and transparent form when the susceptibility of mode i in the absence of

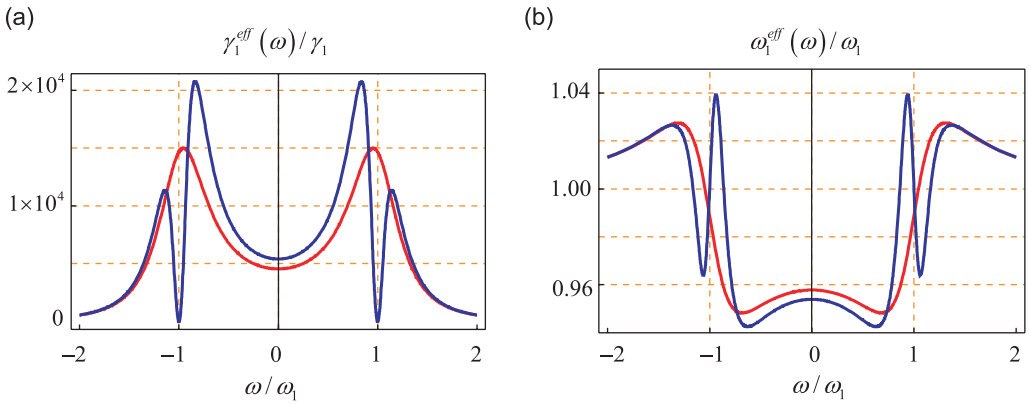

Figure 2. Plot of normalized effective mechanical damping rate (a) and mechanical frequency (b) of the main mode in the absence (red line) and presence (blue line) of a secondary mode as a function of ω/ω_1. The parameters are $\gamma_1/2\pi = \gamma_2/2\pi = 100\,\text{Hz}$, $\omega_1/2\pi = 10\,\text{MHz}$, $\omega_2 = \omega_1$, $m_1 = m_2 = 250\,\text{ng}$, $T = 0.6\,\text{K}$, $L = 0.5\,\text{mm}$, $\kappa = 0.3 \times \omega_1$ and $G_1 = \omega_1/5$. The quantities are plotted in the optimal cooling regime, where $\Delta_{(1)} = \omega_1$ for the independent cooling case and $\Delta_{(2)} = \omega_1$ for the simultaneous cooling case. At $\omega = \omega_1$, the effect of the radiation pressure on the main mode is suppressed owing to the coupling to the secondary mode.

the other mode can be taken as that of a usual resonator with an unmodified resonance frequency and a frequency-independent damping rate given by the net laser cooling rate Γ_i,

$$[\chi_i(\omega)]^{-1} = \frac{1}{\omega_i}\left[\left(\omega_i^2 - \omega^2\right) - \mathrm{i}\omega\Gamma_i\right]. \tag{41}$$

In fact, in this case, inserting equation (41) into (36), one arrives at

$$\gamma_i^{\text{eff}}(\omega) \simeq \gamma_1 + \Gamma_1 \frac{\left[\left(\omega_2^2 - \omega^2\right)^2 + \omega^2\gamma_2\Gamma_2\right]}{\left(\omega_2^2 - \omega^2\right)^2 + \omega^2\Gamma_2^2} \simeq (\gamma_1 + \Gamma_1) - \Gamma_1 \frac{\omega^2\Gamma_2^2}{\left(\omega_2^2 - \omega^2\right)^2 + \omega^2\Gamma_2^2}. \tag{42}$$

Since the effective resonance frequency is not altered, the effective damping of mode 1 in the presence of the second mode is essentially determined by $\gamma_i^{\text{eff}}(\omega_1)$, i.e. equation (42) evaluated at resonance. Therefore, one has that when $\omega_1 = \omega_2$, $\gamma_i^{\text{eff}}(\omega_1) \simeq \gamma_1$, implying that at resonance the second-order scattering processes mediating the interaction between the two mechanical modes completely suppress cooling. This process is a classical destructive interference phenomenon, similar to the classical analogue of electromagnetically induced transparency realized with two coupled oscillators shown in [44]. Another important piece of information provided by equation (42) is that this destructive interference starts affecting cooling when $\delta\omega_{21} < \Gamma_2$, that is, equation (42) shows that the 'bandwidth' within which one has suppression of cooling is given by the effective mechanical damping, modified by the radiation pressure of the cavity, Γ_2.

One can also view the suppression of cooling taking place when the two mechanical modes are resonant in a different way, starting from the interaction Hamiltonian of equation (6), which shows that the cavity mode directly interacts only with the collective coordinate $\sum_j G_0^j q_j$. This

suggests that, in the case of two mechanical modes, it is useful to pass to the effective 'center-of-mass' and 'relative' coordinates

$$q_{\rm cm} = \frac{G_0^1 q_1 + G_0^2 q_2}{[G_0^1]^2 + [G_0^2]^2}, \qquad p_{\rm cm} = \frac{G_0^1 p_1 + G_0^2 p_2}{[G_0^1]^2 + [G_0^2]^2}, \tag{43}$$

$$q_{\rm r} = \frac{G_0^1 q_2 - G_0^2 q_1}{[G_0^1]^2 + [G_0^2]^2}, \qquad p_{\rm r} = \frac{G_0^1 p_2 - G_0^2 p_1}{[G_0^1]^2 + [G_0^2]^2}. \tag{44}$$

With the new coordinates, the free Hamiltonian of the two mechanical modes becomes

$$H_{\rm mech} = \frac{\hbar\omega_{\rm cm}}{2}\left(q_{\rm cm}^2 + p_{\rm cm}^2\right) + \frac{\hbar\omega_{\rm r}}{2}\left(q_{\rm r}^2 + p_{\rm r}^2\right) + \frac{\hbar(\omega_2 - \omega_1) G_0^1 G_0^2}{[G_0^1]^2 + [G_0^2]^2}\left(q_{\rm cm} q_{\rm r} + p_{\rm cm} p_{\rm r}\right), \tag{45}$$

where $\omega_{\rm cm} = \{[G_0^1]^2\omega_1 + [G_0^2]^2\omega_2\}/\{[G_0^1]^2 + [G_0^2]^2\}$ and $\omega_{\rm r} = \{[G_0^1]^2\omega_2 + [G_0^2]^2\omega_1\}/\{[G_0^1]^2 + [G_0^2]^2\}$. This shows that at resonance, $\omega_2 = \omega_1$, the relative coordinate $q_{\rm r}$ is decoupled from the center-of-mass and therefore also from the cavity mode (see equation (6)). As a consequence, it remains in its initial thermal state at the reservoir temperature and it is uncooled. Therefore, even though the center of mass is cooled close to its ground state, the two mechanical modes, 1 and 2, are only negligibly cooled because their steady-state energy is determined by a weighted sum of the center of mass and relative mean energy. If instead $\omega_1 \neq \omega_2$, the relative motion is coupled to the center of mass and the cooling of the latter by the cavity mode is able to partially cool also the relative motion. This 'sympathetic' cooling is more efficient for larger coupling, i.e. for increasing $\omega_2 - \omega_1$, provided both modes are not too far from resonance with the cavity.

4. Entanglement properties of the steady state of the system

From the results of [25] and [27], one can see that in the optimal cooling regime for a single mechanical mode $\Delta_{(1)} \simeq \omega_1$, one has also a significant stationary entanglement between the mechanical and the optical cavity modes, which is also quite robust against temperature [27]. It is therefore interesting to study the entanglement properties of the stationary state of the tripartite system formed by the two close mechanical modes and the cavity mode. In particular, it is interesting to see if each mechanical mode is entangled with the optical mode, as in the single mode case, and also if the common interaction with the cavity mode enables the establishment of purely mechanical entanglement between the two vibrational modes.

The 6×6 steady-state correlation matrix $\mathcal{V}$ defined by equation (28), particularized for the case of two mechanical modes, can be written in terms of blocks of 2×2 matrices as

$$\mathcal{V} = \begin{pmatrix} \mathcal{A}_1 & \mathcal{C}_{12} & \mathcal{D}_1 \\ \mathcal{C}_{12}^{\intercal} & \mathcal{A}_2 & \mathcal{D}_2 \\ \mathcal{D}_1^{\intercal} & \mathcal{D}_2^{\intercal} & \mathcal{B} \end{pmatrix}. \tag{46}$$

In order to quantify the bipartite entanglement of the Gaussian steady state of the three different instances of bipartite systems, we use the logarithmic negativity [45], defined as

$$\mathcal{E}(\mathcal{V}_{\rm bip}) = \max\left\{0, -\ln 2\eta^{-}(\mathcal{V}_{\rm bip})\right\}, \tag{47}$$

where $\mathcal{V}_{\rm bip}$ is a generic 4×4 correlation matrix associated with the bipartite system of interest

$$\mathcal{V}_{\rm bip} \equiv \begin{pmatrix} \mathcal{A} & \mathcal{C} \\ \mathcal{C}^{\intercal} & \mathcal{B} \end{pmatrix}, \tag{48}$$

and $\eta^{-}(\mathcal{V}_{\rm bip})$ is given by [45]

$$\eta^{-}\left(\mathcal{V}_{\rm bip}\right) \equiv \frac{1}{\sqrt{2}}\left(\Sigma\left(\mathcal{V}_{\rm bip}\right) - \sqrt{\Sigma\left(\mathcal{V}_{\rm bip}\right)^{2} - 4\det\mathcal{V}_{\rm bip}}\right)^{1/2}, \tag{49}$$

with $\Sigma(\mathcal{V}_{\rm bip}) \equiv \det\mathcal{A} + \det\mathcal{B} - 2\det\mathcal{C}$. The bipartite state is entangled if and only if $\eta^{-}(\mathcal{V}_{\rm bip}) < 1/2$, which is equivalent to the positive partial transpose (PPT) criterion, a necessary and sufficient entanglement criterion in the case of bipartite Gaussian states [46].

To analyze the entanglement between one of the acoustic modes and the field, it suffices to eliminate the rows and columns that correspond to the other mirror mode from the matrix $\mathcal{V}$ of equation (46). We are left with a 4×4 matrix

$$\mathcal{V}_{f-m} \equiv \begin{pmatrix} \mathcal{A}_{1,2} & \mathcal{D}_{1,2} \\ \mathcal{D}_{1,2}^{\intercal} & \mathcal{B} \end{pmatrix}. \tag{50}$$

We have performed a numerical analysis around the parameter region considered in [27], which is within reach of state-of-the-art experiments (see the caption of figure 3) and for which, in the presence of a single mechanical mode, one has a significant, stationary, optomechanical entanglement.

We find that, similar to what happens for cooling, the entanglement properties of the steady state of the system strongly depend upon the value of the difference between the two mechanical resonance frequencies, $\delta\omega_{21}$. When the two modes are well separated, $\delta\omega_{21} > \Gamma_i$, the presence of the second mode does not affect too much the main mode–cavity field entanglement. Moreover, also the secondary mechanical mode is entangled with the cavity. This is illustrated in figure 3(a), where the optomechanical logarithmic negativity in the single mechanical mode case (red line) is plotted versus the cavity detuning and compared with the corresponding curves for the main mechanical mode (blue) and the secondary mode (green), when both modes are present. Optomechanical entanglement is more fragile than cooling, because in the two-mode case it is always smaller than that with a single mechanical mode.

Figures 3(b) and (c) show that the situation changes drastically when the two mechanical modes become very close in frequency, $\omega_2/\omega_1 \simeq 1$. Both figures show the logarithmic negativity at a fixed detuning, versus the ratio ω_2/ω_1, at zero temperature (b) and at $T = 0.4\,\mathrm{K}$ (c). We see that at zero temperature, the entanglement *increases* around resonance, $\omega_2/\omega_1 = 1$. However, such an entanglement is very fragile with respect to temperature, and vanishes at $T = 0.4\,\mathrm{K}$ (c) for a wide interval around the resonance condition. This behavior can be understood using the arguments in the preceding section. At mechanical resonance, the cavity mode is strongly coupled, and entangled, to the center of mass, and uncoupled from the relative coordinate. Modes 1 and 2 are linear combinations of $q_{\rm cm}$ and $q_{\rm r}$ and therefore their entanglement with the cavity mode is determined by both $q_{\rm cm}$ and $q_{\rm r}$. At $T = 0$, both mode 1 and mode 2 are entangled with the cavity mode, thanks to the cavity–center-of-mass entanglement and because the quantum fluctuations of $q_{\rm r}$ do not significantly affect it. However, as soon as temperature is increased, the thermal fluctuations of the uncoupled coordinate $q_{\rm r}$ kill the entanglement of modes 1 and 2 with the cavity, even though cavity–center-of-mass entanglement is robust against temperature. Finally, the robustness of these optomechanical entanglements against temperature is analyzed in figure 3(d). We see that even though never comparable to the case of a single mechanical mode, provided the frequencies of the two modes are sufficiently far apart, i.e. $\delta\omega_{21} \gtrsim \Gamma_2$ (we have chosen $\omega_2 = 1.5\omega_1$), one has a regime in which the two modes are simultaneously entangled, and this persists up to a few kelvins.

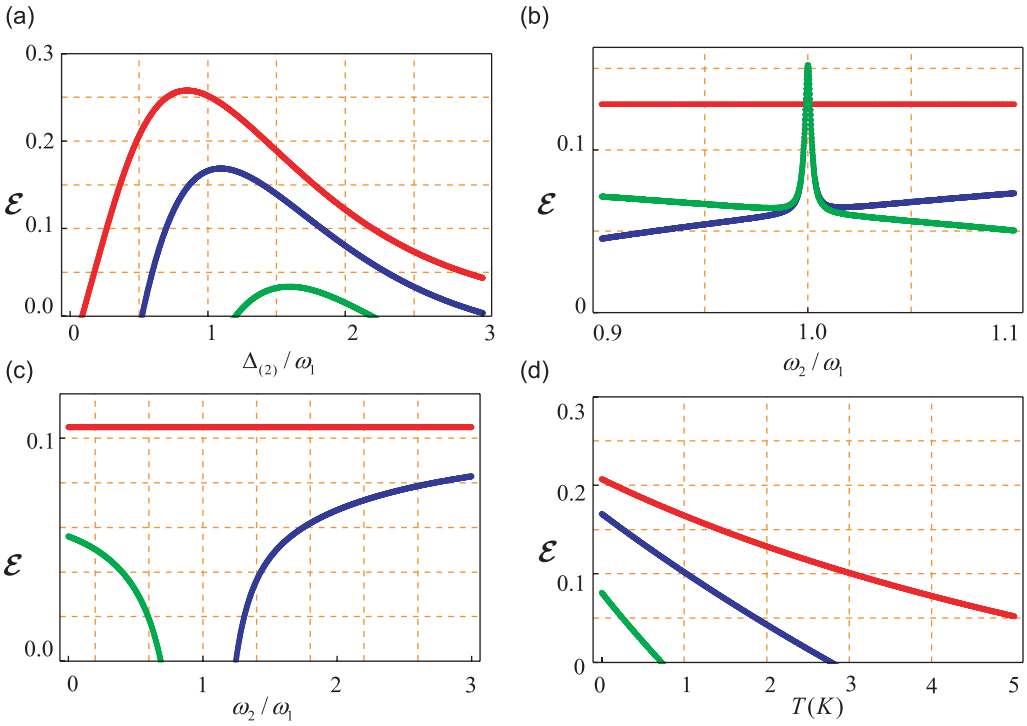

Figure 3. Optomechanical entanglement. (a) Mirror-field entanglement in the absence of secondary mechanical modes (red line) is plotted versus normalized detuning $\Delta_{(2)}/\omega_1$ and compared with main mode–field entanglement (blue) and secondary mode–field entanglement (green). The parameters are $\gamma_1/2\pi = \gamma_2/2\pi = 100\,\text{Hz}$, $\omega_1/2\pi = 10\,\text{MHz}$, $\omega_2 = 1.5 \times \omega_1$, $m_1 = m_2 = 250\,\text{ng}$, $T = 0.4\,\text{K}$, $\kappa = 0.9 \times \omega_1$ and $G_1 = \omega_1$. (b) Enhancement of acousto-optical entanglement at zero temperature for close modes. The red line shows the value of the negativity of the main mode–field entanglement in the absence of the secondary mode, while the blue and green curves show the behavior of the logarithmic negativity in the two-mode case, when ω_1 is fixed and ω_2 is swept around ω_1. In this case, $G_1 \simeq 0.6\omega_1$ and we have fixed $\Delta_{(2)} = \omega_1$. (c) The enhancement shown in (b) is lost as soon as the temperature increases. Here, the environment is at $T = 0.4\,\text{K}$ and the secondary mode frequency is varied between $0.5 \times \omega_1$ and $3\omega_1$. (d) Temperature robustness of entanglement in the collective case (blue and green lines for main and secondary mode respectively) compared to the independent case (red line). Here $\omega_2 = 1.5 \times \omega_1$, and we have chosen $\Delta_{(2)} = \omega_2$ such that a simultaneous entanglement regime is obtained.

One can also check if the two mechanical modes, even though not directly interacting, can become entangled at the steady state, thanks to the common interaction with the cavity mode. Eliminating the entries in $\mathcal{V}$ that correspond to the cavity field, one is left with an all mechanical correlation matrix

$$\mathcal{V}_{m-m} \equiv \begin{pmatrix} \mathcal{A}_1 & \mathcal{C}_{12} \\ \mathcal{C}_{12}^{\mathsf{T}} & \mathcal{A}_2 \end{pmatrix}. \tag{51}$$

A numerical analysis of $\mathcal{E}(\mathcal{V}_{m-m})$ in a parameter regime around the region of optimal cooling, i.e. that of figures 1 and 3, shows no entanglement between the two mechanical modes, even

when they are both strongly entangled with the same cavity field. Nonzero but extremely weak bipartite mechanical entanglement can be instead obtained in a regime where the oscillators are heavily damped and the cavity finesse is very high ($\kappa \sim \gamma_{1,2} < \omega_{1,2}$). This is consistent with the results of [47], where bipartite entanglement between two different macroscopic oscillators is analyzed. In fact, the present system is analogous to that considered in [47], with the center of mass $q_{\rm cm}$ of the two modes here playing the same role as the relative coordinate of [47]. As already shown in [47], purely mechanical entanglement is very fragile with respect to temperature and vanishes as soon as the occupancy of one of the modes is of the order of one.

5. Classification of tripartite entanglement

The tripartite system under study can have various forms of tripartite entanglement, and it is therefore important to classify the entanglement possessed by the steady state of the system. We determine the entanglement class of the system state by applying the results of [35], which has provided a necessary and sufficient criterion for the determination of the class in the case of tripartite CV Gaussian states and which is directly computable. This classification criterion is mostly based on the nonpositive partial transposition (NPT) criterion proved in [48], which is necessary and sufficient for $1 \times N$ bipartite CV Gaussian states. The NPT criterion of [48] can be expressed in terms of the symplectic matrix

$$\mathcal{J} = \bigoplus_{i=1}^{3} J_i, \quad J_i = \begin{pmatrix} 0 & 1 \\ -1 & 0 \end{pmatrix}, \quad i = 1, 2, 3 \tag{52}$$

and of the partial transposition transformation Λ_k, acting on system k only. Transposition is equivalent to time reversal and therefore in phase space is equivalent to changing the sign of the momentum operators. The NPT criterion states that a $1 \times N$ CV Gaussian state is separable if and only if the 'test matrix' $\tilde{V}_k = \Lambda_k V \Lambda_k + \mathrm{i}\mathcal{J}/2 \geqslant 0$. Therefore, by evaluating the sign of the eigenvalues of the three possible matrices $\tilde{V}_k$, and using the NPT criterion, one can discriminate between the various entanglement classes. The results of this analysis are shown in figure 4. We find again that the properties of the steady state crucially depend upon the comparison between the difference between the two mechanical frequencies $\delta\omega_{21}$ and the effective mechanical damping Γ_j. When $\delta\omega_{21} > \Gamma_j$, the system is a fully tripartite state in a wide-parameter region around the optimal cooling regime studied here, because the minimum eigenvalues for each bipartition are always negative (see figure 4(a)). Instead, when the two frequencies are very close to each other ($\delta\omega_{21} < \Gamma_j$), we see from figure 4(b) that two eigenvalues, those corresponding to isolating a mechanical mode from the other two modes, are always positive, in a wide interval for the detunings. This means that the steady state is of *class 3*, i.e. a two-mode biseparable state [49], which is separable when the bipartite splits corresponding to isolating one of the two mechanical modes are considered, but inseparable when the cavity mode is split from the rest. This can be understood by recalling again that when $\omega_1 = \omega_2$, the cavity mode is strongly coupled with the center-of-mass coordinate $q_{\rm cm}$ and decoupled from the relative coordinate $q_{\rm r}$. The tripartite biseparable state manifests the fact that the cavity is entangled with the center of mass of the two oscillators. Entanglement is lost when one of the two mechanical modes is traced out and one restricts to bipartite entanglement only.

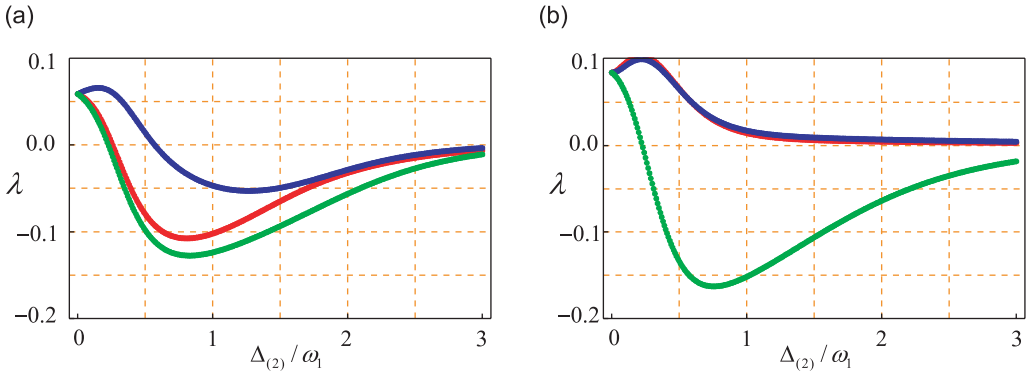

Figure 4. Analysis of tripartite entanglement in the limit of well-separated mechanical modes $\omega_2 = 1.5 \times \omega_1$ (a), and closely spaced modes $\omega_2 = 1.01 \times \omega_1$ (b). The minimum eigenvalues after partial transposition with respect to the main mode (red line), secondary mode (blue line) and field (green line) are plotted versus normalized detuning $\Delta_{(2)}/\omega_1$ for a set of parameters $\gamma_1/2\pi = \gamma_2/2\pi = 100\,\text{Hz}$, $\omega_1/2\pi = 10\,\text{MHz}$, $m_1 = m_2 = 250\,\text{ng}$, $T = 0.4\,\text{K}$, $L = 0.5\,\text{mm}$, $\kappa = 0.5 \times \omega_1$ and $G_1 = 0.7 \times \omega_1$. For a large range of detunings, for well-separated modes, the total system is in a fully inseparable, tripartite-entangled state (a), whereas for close frequencies the resulting state is two-mode biseparable (b).

6. Conclusions

We have analyzed the effect of the radiation pressure of a cavity field mode on two vibrational modes of a mirror of a Fabry–Perot cavity which are near in frequency and both within the detection bandwidth. We have considered the effect of the second mechanical mode both on ground state cooling via the back-action of the cavity mode, and on the optomechanical entanglement at the steady state. We have seen that the result crucially depends upon the difference between the two mechanical resonance frequencies. If this difference is larger than the effective bandwidth of the mechanical oscillators, given by the effective damping, the second mode not only does not affect cooling, but it is simultaneously cooled together with the main mode. Under the same condition, each mode is entangled with the cavity mode and the steady state is a fully tripartite entangled state. Instead, when the two mechanical frequencies are very close to each other, cooling is destroyed by a classical interference effect and both modes are uncooled. In this condition, each mechanical mode is entangled with the cavity mode at zero temperature, but such an entanglement is extremely fragile with respect to temperature. Moreover, in the same regime, the steady state is a two-mode biseparable state which is inseparable only when the cavity mode is split from the rest. In these parameter regimes, the mechanical modes instead are never entangled; they can become entangled only for high-finesse cavities, but the resulting entanglement vanishes at extremely low temperatures.

Acknowledgment

This work was supported by the European Commission through the program QAP.

References

[1] Schwab K C and Roukes M L 2005 *Phys. Today* **58** 36
[2] Friedsam C *et al* 2003 *J. Phys.: Condens. Matter* **15** S1709
[3] Rugar D *et al* 2004 *Nature* **430** 329
[4] Ekinci K L, Yang Y T and Roukes M L 2004 *J. Appl. Phys.* **95** 2682
[5] Braginsky V B and Khalili F Ya 1992 *Quantum Measurements* (Cambridge: Cambridge University Press)
[6] Marshall W, Simon C, Penrose R and Bouwmeester D 2003 *Phys. Rev. Lett.* **91** 130401
[7] LaHaye M D *et al* 2004 *Science* **304** 74
[8] Gigan S, Böhm H, Paternostro M, Blaser F, Langer G, Hertzberg J, Schwab K, Bäuerle D, Aspelmeyer M and Zeilinger A 2006 *Nature* **444** 67
[9] Arcizet O, Cohadon P-F, Briant T, Pinard M and Heidmann A 2006 *Nature* **444** 71
[10] Schliesser A, Del'Haye P, Nooshi N, Vahala K J and Kippenberg T J 2006 *Phys. Rev. Lett.* **97** 243905
[11] Corbitt T, Chen Y, Innerhofer E, Müller-Ebhardt H, Ottaway D, Rehbein H, Sigg D, Whitcomb S, Wipf C and Mavalvala N 2007 *Phys. Rev. Lett.* **98** 150802
[12] Thompson J D, Zwickl B M, Jayich A M, Marquardt F, Girvin S M and Harris J G E 2008 *Nature* **452** 72
[13] Schliesser A, Rivière R, Anetsberger G, Arcizet O and Kippenberg T J 2008 *Nat. Phys.* **4** 415
[14] Cohadon P F, Heidmann A and Pinard M 1999 *Phys. Rev. Lett.* **83** 3174
[15] Arcizet O, Cohadon P-F, Briant T, Pinard M, Heidmann A, Mackowski J M, Michel C, Pinard L, Francais O and Rousseau L 2006 *Phys. Rev. Lett.* **97** 133601
[16] Kleckner D and Bouwmeester D 2006 *Nature* **444** 75
[17] Poggio M, Degen C L, Mamin H J and Rugar D 2007 *Phys. Rev. Lett.* **99** 017201
[18] Corbitt T, Wipf C, Bodiya T, Ottaway D, Sigg D, Smith N, Whitcomb S and Mavalvala N 2007 *Phys. Rev. Lett.* **99** 160801
[19] Mancini S *et al* 1998 *Phys. Rev. Lett.* **80** 688
[20] Braginsky V B *et al* 2001 *Phys. Lett.* A **287** 331
[21] Courty J-M *et al* 2001 *Eur. Phys. J.* D **17** 399
[22] Vitali D, Mancini S, Ribichini L and Tombesi P 2002 *Phys. Rev.* A **65** 063803
Vitali D, Mancini S, Ribichini L and Tombesi P 2003 *J. Opt. Soc. Am.* B **20** 1054
Vitali D, Mancini S, Ribichini L and Tombesi P 2004 *Phys. Rev.* A **69** 029901
[23] Wilson-Rae I *et al* 2007 *Phys. Rev. Lett.* **99** 093901
[24] Marquardt F *et al* 2007 *Phys. Rev. Lett.* **99** 093902
[25] Genes C, Vitali D, Tombesi P, Gigan S and Aspelmeyer M 2008 *Phys. Rev.* A **77** 033804
[26] Dantan A *et al* 2008 *Phys. Rev.* A **77** 011804
[27] Vitali D *et al* 2007 *Phys. Rev. Lett.* **98** 030405
Paternostro M *et al* 2007 *Phys. Rev. Lett.* **99** 250401
[28] Mancini S *et al* 2002 *Phys. Rev. Lett.* **88** 120401
[29] Zhang J, Peng K and Braunstein S L 2003 *Phys. Rev.* A **68** 013808
[30] Pinard M *et al* 2005 *Europhys. Lett.* **72** 747
[31] Bhattacharya M, Giscard P L and Meystre P 2008 *Phys. Rev.* A **77** 030303
[32] Mancini S, Vitali D and Tombesi P 2003 *Phys. Rev. Lett.* **90** 137901
[33] Pirandola S, Vitali D, Tombesi P and Lloyd S 2006 *Phys. Rev. Lett.* **97** 150403
[34] Ludwig M, Neuenhahn C, Metzger C, Ortlieb A, Favero I, Karrai K and Marquardt F 2007 *Preprint* 0711.2661v2 [cond-mat.mes-hall]
[35] Giedke G, Kraus B, Lewenstein M and Cirac J I 2001 *Phys. Rev.* A **64** 052303
[36] Law C K 1995 *Phys. Rev.* A **51** 2537
[37] Pinard M, Hadjar Y and Heidmann A 1999 *Eur. Phys. J.* D **7** 107
[38] Gardiner C W and Zoller P 2000 *Quantum Noise* (Berlin: Springer)
[39] Giovannetti V and Vitali D 2001 *Phys. Rev.* A **63** 023812

[40] Benguria R and Kac M 1981 *Phys. Rev. Lett.* **46** 1
[41] Parks P C and Hahn V 1993 *Stability Theory* (New York: Prentice Hall)
[42] Gradshteyn I S and Ryzhik I M 1980 *Tables of Integrals, Series and Products* (Orlando, FL: Academic) p 1119
[43] Dorsel A, McCullen J D, Meystre P, Vignes E and Walther H 1983 *Phys. Rev. Lett.* **51** 1550
Gozzini A, Maccarone F, Mango F, Longo I and Barbarino S 1985 *J. Opt. Soc. Am.* B **2** 1841
[44] Garrido Alzar C L, Martinez M A G and Nussenzveig P 2002 *Am. J. Phys.* **70** 37
[45] Eisert J 2001 *PhD Thesis* University of Potsdam
Vidal G and Werner R F 2002 *Phys. Rev.* A **65** 032314
Adesso G *et al* 2004 *Phys. Rev.* A **70** 022318
[46] Duan L M *et al* 2000 *Phys. Rev. Lett.* **84** 2722
Simon R 2000 *Phys. Rev. Lett.* **84** 2726
[47] Vitali D, Mancini S and Tombesi P 2007 *J. Phys. A: Math. Theor.* **40** 8055
[48] Werner R F and Wolf M M 2001 *Phys. Rev. Lett.* **86** 3658
[49] Dür W, Cirac J I and Tarrach R 1999 *Phys. Rev. Lett.* **83** 3562
Dür W and Cirac J I 2000 *Phys. Rev.* A **61** 042314